JACS
JOURNAL OF THE AMERICAN CHEMICAL SOCIETY

ARTICLE

pubs.acs.org/JACS

Photosynthetic Light-Harvesting Is Tuned by the Heterogeneous Polarizable Environment of the Protein

Carles Curutchet,*[,†,‡] Jacob Kongsted,[§] Aurora Muñoz-Losa,[⊥] Hoda Hossein-Nejad,[#] Gregory D. Scholes,[‡] and Benedetta Mennucci[⊥]

[†]Institut de Química Computacional and Departament de Química, Universitat de Girona, Campus Montilivi 17071 Girona, Spain

[‡]Department of Chemistry, 80 St. George Street, Institute for Optical Sciences, and Centre for Quantum Information and Quantum Control, University of Toronto, Toronto, Ontario, M5S 3H6 Canada

[§]Department of Physics and Chemistry, University of Southern Denmark, Campusvej 55, DK-5230 Odense M, Denmark

[⊥]Dipartimento di Chimica e Chimica Industriale, Università di Pisa, via Risorgimento 35, 56126 Pisa, Italy

[#]Department of Physics, 60 St. George Street, Institute for Optical Sciences, and Centre for Quantum Information and Quantum Control, University of Toronto, Toronto, Ontario, M5S 1A7 Canada

Supporting Information

ABSTRACT: In photosynthesis, special antenna proteins that contain multiple light-absorbing molecules (chromophores) are able to capture sunlight and transfer the excitation energy to reaction centers with almost 100% quantum efficiencies. The critical role of the protein scaffold in holding the appropriate arrangement of the chromophores is well established and can be intuitively understood given the need to keep optimal dipole−dipole interactions between the energy-transferring chromophores, as described by Förster theory more than 60 years ago. However, the question whether the protein structure can also play an active role by tuning such dipole−dipole interactions has not been answered so far, its effect being rather crudely described by simple screening factors related to the refractive index properties of the system. Here, we present a combined quantum chemical/molecular mechanical approach to compute electronic couplings that accounts for the heterogeneous dielectric nature of the protein−solvent environment in atomic detail. We apply the method to study the effect of dielectric heterogeneity in the energy migration properties of the PE545 principal light-harvesting antenna of the cryptomonad *Rhodomonas* CS24. We find that dielectric heterogeneity can profoundly tune by a factor up to ∼4 the energy migration rates between chromophore sites compared to the average continuum dielectric view that has historically been assumed. Our results indicate that engineering of the local dielectric environment can potentially be used to optimize artificial light-harvesting antenna systems.

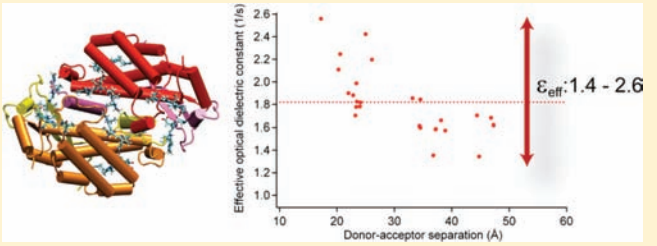

INTRODUCTION

Light-harvesting proteins are used in photosynthesis to capture incident sunlight and funnel its energy to the reaction centers.[1] Recent work has discovered that a contribution to the dynamics of energy transfer within some photosynthetic proteins involves quantum-coherence.[2−4] Those reports have inspired many theoretical studies, where the critical role played by the environment has been highlighted. For example, decoherence and energy transfer are caused by coupling of electronic transitions to the stochastic fluctuations of the environment. The frequency spectrum of the environment (spectral density) is therefore an important quantity. Equally important is the way the electronic coupling between molecules is influenced by the environment. This "off-diagonal" effect is less studied. The details of such chromophore−environment interactions are not well-known for photosynthetic proteins. Moreover, while the heterogeneity of a protein is well recognized, how that influences energy transfer by tuning the electronic coupling between molecules is yet to be ascertained. In the present report we describe how heterogeneity of protein structure and hence dielectric environment can tune energy transfer dynamics profoundly. We find that energy transfer times between pairs of molecules in a photosynthetic light-harvesting complex from cryptophyte algae are tuned by a factor up to ∼4 relative to expectations based on the average dielectric environment.

In a recent work we addressed the issue of solvent screening of electronic couplings in energy transfer by using quantum chemical calculations with explicit account of a polarizable continuum environment.[5,6] While it is well-known that screening reduces

Received: November 9, 2010
Published: February 15, 2011

dx.doi.org/10.1021/ja110053y | *J. Am. Chem. Soc.* 2011, 133, 3078–3084

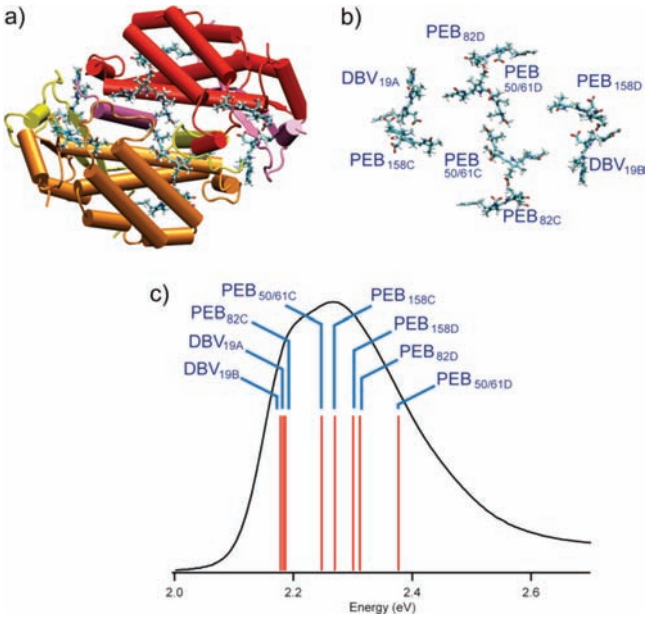

Figure 1. (a) Structure of the PE545 light-harvesting complex. (b) Detailed view of the eight light-absorbing bilin molecules. (c) Electronic absorption spectrum of the isolated PE545 protein in aqueous buffer (294 K) with approximate absorption peaks corresponding to the bilin molecules.[8].

energy transfer rates (by a factor of up to ~4), we found that the screening also depends strongly on the separation and orientation of the chromophores. However, the polarizability within a protein is remarkably heterogeneous. Does that mean that energy transfer between pairs of molecules can be tuned by the nature of the protein in their immediate vicinity? To address this question we have developed a method to calculate electronic couplings between molecules where screening by the protein environment is accounted for with atomic resolution.[7] The method, we term MMPol, uses molecular dynamics simulations to generate manifestations of the environment which are then included in a quantum mechanical calculation of electronic excited states and electronic couplings involving the chromophores embedded in the protein. Thus, the aim of the simulations is not to follow energy transfer dynamics but rather to sample the ground-state ensemble of the system in order to estimate electronic couplings corresponding to the ground-state configuration.

Here we study the principal light-harvesting antenna protein, phycoerythrin PE545, of the cryptomonad *Rhodomonas* CS24 (see Figure 1). Cryptomonads, or cryptophytes, are a phylum of algae that are important primary producers in both marine and freshwater environments. Surprisingly, even though cryptophytes possess fewer varieties of antenna proteins than some organisms, and despite large average center-to-center separations of chromophores in their antennae (about twice that of the major light-harvesting antenna from higher plants), they exhibit maximal photosynthetic activity at very low light intensities, ca. 50 μmol/m^2/s of photons,[9,10] compared to other classes, such as the green alga *Chlorella* sp., 179 μmol/m^2/s.[9] In general, it is of interest to elucidate the optimizations that have evolved to make cryptophyte antenna proteins so efficient.

MMPol calculations were performed for a series of molecular structures extracted from a classical molecular dynamics (MD) simulation of the PE545 system at room temperature, thus allowing us to explore the magnitude of the fluctuations in the effective dielectric properties experienced by the chromophores. In order to obtain insights into the relative screening caused by the protein versus the surrounding water, the calculations were performed for three model systems: First we only accounted for the protein environment, second we included the protein and biological water, and finally we examined the full protein−water system. The MMPol atomistic results are complemented with an analogous method based on a continuum dielectric description of the environment.[6,11] Comparing the latter results to the MMPol calculations allows us to show how the heterogeneous dielectric properties of the PE545 protein can modify the local screening of electronic couplings between the bound chromophores.[1,12]

In Förster theory, it is common to describe the transfer rate by defining a critical Förster radius, R_0, at which the transfer efficiency is 50%. Dielectric screening of the donor−acceptor interaction is contained in R_0 and becomes visible if we define a critical Förster radius, R_0', corresponding to transition dipoles interacting in vacuum:[13]

$$k = \frac{1}{\tau_D}\left(\frac{R_0^6}{R^6}\right) = \frac{1}{\tau_D} s^2 \left(\frac{R_0'^6}{R^6}\right) \quad (1)$$

where τ_D is the lifetime of the donor excited state in the absence of the acceptor, and s is the dielectric screening factor. In the following we will address effective dielectric constants (ε_{eff}) for energy transfer, defined as the inverse screening factor ($s = 1/\varepsilon_{\text{eff}}$), as these provide a more intuitive link to the global optical dielectric permittivity of the environment, i.e., the square of the refractive index.

Atomistic MMPol results were averaged over 141 structures extracted from the molecular dynamics simulation of the complex, whereas continuum model results were obtained from the arrangement of the chromophores as found in the ultrahigh resolution crystal structure.[14] For each structure, we first computed the first low-lying $\pi \rightarrow \pi^*$ excited state of the 8 bilin chromophores in PE545 and subsequently calculated all the corresponding electronic couplings between them (see Methods for details). All calculations were performed at the configuration interaction with singles (CIS) level of theory using the 6-31G basis set. For each structure, MMPol calculations are obtained for three model systems: the isolated protein, the protein plus biological water, and the full protein−water system. These calculations represent a total of ~3400 excited states and ~11900 electronic coupling calculations, in all cases fully accounting for mutual polarization between the chromophores and the environment.

METHODS

Molecular Dynamics Simulations. The simulation system was based on the X-ray crystal structure of PE545 reported at ultrahigh 0.97 Å resolution (Protein Data Bank ID code 1XG0).[14,15] Protonation states of all titratable residues were explored by computing the corresponding pK_as at neutral pH using the automated H++ server,[16−18] indicating a standard ionization state for all residues. All bilin chromophores were modeled having the two central pyrrole rings in their protonated form, as suggested by ultrahigh resolution data.[14] The system was solvated in a pre-equilibrated TIP3P[19] water box (a truncated octahedron with a buffer zone of 12 Å) using the Leap module of the Amber9 suite of programs.[20] The protein and the chromophores were described using the parm99SB[21,22] and the GAFF[23] AMBER force fields,

dx.doi.org/10.1021/ja110053y |J. Am. Chem. Soc. 2011, 133, 3078–3084

respectively. The final system (see Supporting Information for further details), which contained 58131 atoms, was first energy-minimized for 2000 steps of steepest descent plus 8000 steps of conjugate gradient and then gradually thermalized by running five 20-ps molecular dynamics (MD) simulations at constant volume to increase the temperature up to 298 K. Subsequently, a 10-ns MD simulation at constant pressure (1 atm) and temperature (298 K) was carried out using standard coupling schemes. All runs were performed with Amber9[20] using SHAKE to restrain all bonds involving hydrogen, an integration time step of 1 fs, periodic boundary conditions, the Particle Mesh Ewald approach to deal with long-range electrostatics, and a nonbonded cutoff equal to 8 Å. Along the MD simulation, the positional root-mean square deviation determined for the protein backbone with respect to the initial crystal structure was found to be <1.5 Å. From the trajectory, a total of 141 snapshots extracted every 50 ps during the last 7 ns were considered for QM/MM calculations.

Parameterization of the Force Field for MMPol Calculations. In the MMPol calculations the protein and solvent surroundings were described using atom centered charges and isotropic polarizabilities. The force-field has been calculated following the method outlined in ref 24. In summary, the protein is cut into single-residues each caped with $COCH_3$ and $NHCH_3$ groups. These residues are then subjected to separate QM calculations of the force-field parameters. The localized polarizabilities were calculated at the DFT(B3LYP)/aug-cc-pVDZ level using the LoProp[25] approach as implemented in the Molcas quantum chemistry program[26] whereas the partial point charges were obtained from DFT(B3LYP)/cc-pVTZ ESP calculations followed by RESP fittings as implemented in the Gaussian09[27] and Amber9[20] programs, respectively. We calculate the charges and polarizabilities for the crystal structure and used these values for each snapshot extracted from the MD simulations. The parameters for water, derived using the same strategy, were taken from ref 7.

MMPol and Continuum Electronic Coupling Calculations. The MMPol method relies on a mixed quantum mechanics/molecular mechanics (QM/MM) scheme, where the chromophores are described at the quantum mechanical level whereas the protein−solvent environment is described through a classical polarizable force field. Within this framework, the effective Hamiltonian includes the contributions from the MM residual charges, as well as a mutual account of chromophore−environment polarization.[7,28] The latter is iterated to self-consistency using the appropriate perturbed electronic density of the chromophores. The continuum method,[11] based on the Polarizable Continuum Model (PCM),[29] also describes the chromophores quantum-mechanically and accounts for mutual chromophore−environment polarization, but in this case the protein−water surroundings are described as a continuum dielectric medium. In both cases, we first calculate the first low-lying $\pi\rightarrow\pi^*$ excited state of the eight bilin chromophores in PE545 including MMPol or PCM environment effects, store the corresponding transition densities, and subsequently calculate all electronic couplings between them. In both methods, the electronic coupling, to first-order, writes:

$$V = V_s + V_{\text{explicit}} \tag{2}$$

where V_s describes the interaction between donor−acceptor transition densities and V_{explicit} describes the explicit environment-mediated contribution to the electronic coupling, which typically counteracts the V_s term thus leading to an overall environment screening effect. The screening factor and effective dielectric constants for energy transfer are then defined as:

$$s = \frac{1}{\varepsilon_{\text{eff}}} = \frac{V_s + V_{\text{explicit}}}{V_s} \tag{3}$$

Calculations corresponding to the protein plus biological water system were performed by including internal and bound waters within 3 Å of the protein or bilin atoms. In a calculation of the electronic coupling for a specific pair the rest of the chromophores were described at the same level as the protein, i.e., through atom-centered charges and isotropic polarizabilities. In PCM calculations, the protein−water environment was modeled as a dielectric continuum with a relative static dielectric constant of 15 and optical dielectric constant of 2.[30] PCM cavities enclosing the chromophores were obtained in terms of interlocking spheres centered on selected nuclei. The chosen radii were obtained by applying the United Atom Topological Model to the atomic radii of the UFF force field[31] as implemented in the Gaussian 09 code. All PCM and MMPol calculations have been performed using a locally modified version of Gaussian09.[27]

Energy Transfer Rates. We compute the interchromophore transfer rates by adopting a model in which energy transfer is regarded as transitions among the excitonic eigenstates mediated by the vibrational bath.[32] In this formulation exciton delocalization gives the transfer process a collective nature, thereby enhancing the rate of long-range energy transfer. The dynamics of a multichromophoric system under the influence of a phonon bath may be described via the spin-boson Hamiltonian

$$H = -\sum_{mn} J_{mn} a_m^\dagger a_n + \sum_{n,k} a_n^\dagger a_n [\varepsilon_n + \phi_{nk}\omega_k (b_k^\dagger + b_k)] + \sum_k \omega_k b_k^\dagger b_k \tag{4}$$

where J_{mn} is the electronic coupling between the sites m and n, $\{a_n^\dagger, a_n\}$ are the molecular raising and lowering operators for site n, ε_n is the electronic transition energy at site n, $\{b_k^\dagger, b_k\}$ are the bosonic creation and annihilation operators for mode k of the bath, ϕ_{nk} is a dimensionless displacement quantifying the exciton−phonon coupling between site n and mode k, and ω_k are the bath frequencies. Following the approach of Pereverzev and Bittner,[33] we diagonalize the electronic part of the Hamiltonian and apply the same transformation to the exciton−phonon part. The transformed Hamiltonian is found to be

$$\bar{H} = \sum_\alpha E_\alpha A_\alpha^\dagger A_\alpha + \sum_{\alpha\beta k} g_{\alpha\beta k} A_\beta^\dagger A_\alpha (b_k + b_k^\dagger) + \sum_k \omega_k b_k^\dagger b_k \tag{5}$$

where E_α are the eigenstates energies, $\{A_\alpha^\dagger, A_\alpha\}$ are the creation and annihilation operators in the exciton basis, $g_{\alpha\beta k} = \sum_i T_{i\alpha} T_{i\beta} \omega_k \phi_{ik}$ and T is the operator that diagonalizes the electronic part of the Hamiltonian. The transfer rate between two eigenstates is given by the integral of the associated memory kernel, that is

$$k_{\alpha\beta}(t) = \int_0^t d\tau\, G_{\alpha\beta}(\tau) \tag{6}$$

where $k_{\alpha\beta}(t)$ is the transfer rate between two eigenstates $|\alpha\rangle$ and $|\beta\rangle$. The associated memory kernel $G_{\alpha\beta}(t)$, is given by

$$G_{\alpha\beta}(t) = 2Re\left\{ e^{i\bar{\Omega}_{\alpha\beta} t} \sum_{kq} \langle M_{\alpha\beta k}(t)\, M_{\beta\alpha q}(0)\rangle \right\} \tag{7}$$

$$M_{\beta\alpha k} = g_{\alpha\beta k}\left(b_k^\dagger + b_k - \frac{2g_{\alpha\alpha k}}{\omega_k}\right) exp\left\{ \sum_q \frac{g_{\alpha\alpha q} - g_{\beta\beta q}}{\omega_q}(b_q^\dagger - b_q) \right\} \tag{8}$$

where $\tilde{\Omega}_{\alpha\beta}$ is the frequency difference between the two eigenstates, and the angled brackets indicate an averaging with respect to the phonon modes. The transfer rate in the steady state can be obtained by setting the upper limit of the integral in eq 6 to infinity. We use this procedure to obtain the transfer rates between all chromophore pairs for the three estimates of the PE545 Hamiltonian (total system, system plus biological

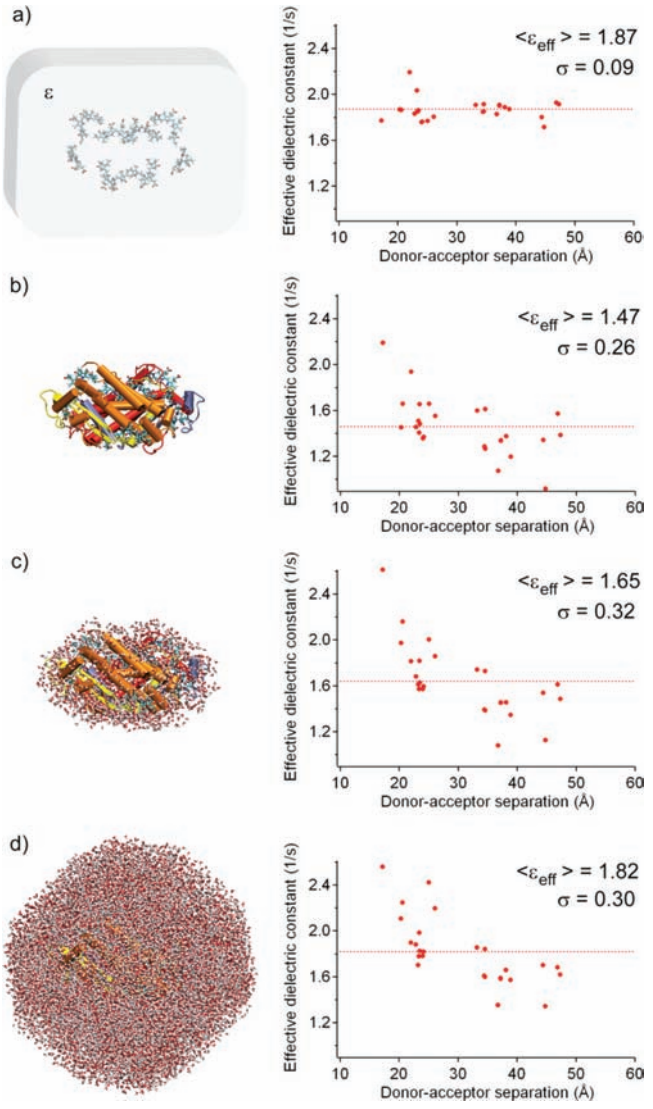

Figure 2. Effective optical dielectric constants (inverse environment screening effect) for electronic energy transfer experienced by the chromophore pairs in the PE545 complex as predicted by a continuum dielectric or an atomistic description of the protein and water environment. Continuum results (a) are obtained based on the ultrahigh resolution crystal structure of PE545, whereas MMPol results are averaged for a set of structures extracted from a molecular dynamics trajectory and obtained for the isolated protein (b), the protein and the bound waters (c), or the full protein−water environment (d). In each case, the dielectric constant averaged over the multiple chromophore pairs in PE545 as well as the corresponding standard deviation is indicated.

waters, and system with no biological waters). In each scenario the transfer rates are computed for 141 temporal snapshots of the Hamiltonian. The diagonal energies remain constant in all realizations (model E from ref 8). The modes of the vibrational bath consist of 14 discrete oscillator modes[8] and an additional discrete mode obtained by fitting to room temperature and 77 K fluorescence spectra.[32]

RESULTS AND DISCUSSION

The values of effective optical dielectric permittivities obtained from the atomistic MMPol or the continuum methods for the pigment pairs in the PE545 complex are shown in Figure 2. The continuum dielectric method indicates a size-dependent screening[5] that yields an average effective permittivity for energy transfer of $\langle\varepsilon_{\mathrm{eff}}\rangle = 1.87$. On the other hand, the atomistic methods give averaged values in the range 1.47−1.82 with the isolated protein model showing the smallest $\langle\varepsilon_{\mathrm{eff}}\rangle$. The other two atomistic descriptions allow for a detailed analysis of the role of the bound and the external waters in the system. Inclusion of the water bound to the protein surface leads to an average 12% increase of the permittivity. A further 12% increase is obtained by the addition of the surrounding bulk waters. This increase is explained by the fact that water now occupies voids in the protein, thus necessarily increasing the global permittivity of the system. When all water molecules are accounted for, the $\langle\varepsilon_{\mathrm{eff}}\rangle = 1.82$ value closely resembles that obtained with the continuum approach. Thus, if we focus on an average picture, the continuum description compares well with the more accurate description obtained using a full atomistic approach.

The agreement between results averaged over all chromophore pairs in the antenna complex can be explained if we analyze the components of each model. In the continuum method, the screening is described in terms of a set of induced charges spread on the cavities embedding the chomophores inside the dielectric medium. These charges represent the polarization of the environment caused by the electronic transition in the donor, and they are calculated in terms of the square of the refractive index used to represent the mixed protein−water environment (namely 2). In the atomistic approaches, instead, the screening is calculated in terms of induced dipoles still originated by the electronic transition in the donor. This time, however, these induced dipoles are determined by the atomic polarizabilities used to mimic the protein (and the water). If we evaluate the square of the refractive index from such polarizabilities (see Supporting Information for details) we obtain $\varepsilon_{\mathrm{opt}} = 2.27$ for the PE545 crystal structure. Thus, it is reasonable to expect that the global optical permittivity of the system is in between the $\varepsilon_{\mathrm{opt}} \approx 2.3$ and $\varepsilon_{\mathrm{opt}} \approx 1.8$ values of the protein and water regions, respectively, i.e., similar to $\varepsilon_{\mathrm{opt}} = 2$ assumed in the continuum model calculations. For instance, if we evaluate $\varepsilon_{\mathrm{opt}}$ for a structure extracted from the MD simulation, the inclusion of bound waters lowers the $\varepsilon_{\mathrm{opt}}$ value from 2.35 to 2.21. The continuum and the atomistic descriptions contain the same ingredients and necessarily give similar results on average.[34]

A continuum dielectric description condenses the multiple responses of the many amino acids and waters participating in the process into a simple parameter, the optical dielectric permittivity adopted in the model. This simplicity, however, precludes elucidation of any specific influence the protein structure might confer on dielectric screening. The catalogue of natural amino acids has a remarkable variety in their degree of polarization,[35] so a natural question arises: can the protein structure use this catalogue to engineer optimized dielectric responses in photosynthetic complexes? If so, to what extent is such an optimization possible?

The results in Figure 2 demonstrate that remarkable variation of the dielectric response of the environment experienced by the bilin pairs in PE545 is indeed possible. Whereas effective permittivities for energy transfer obtained using a continuum dielectric description of the protein plus water environment span a range of values 1.72−2.20, the parallel protein plus water atomistic description provides a significantly broader range from 1.35 to 2.57. Note here that the range of values predicted by the continuum dielectric model arises from the different orientation and distances between the interacting molecules.[5,6] Furthermore, the similar spread of the atomistic results, which persists with or without the

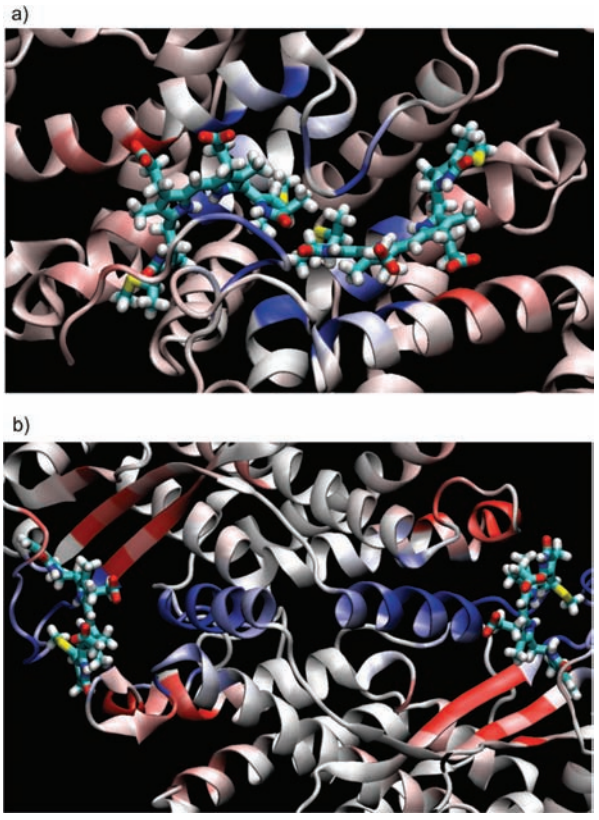

Figure 3. Graphical representation of PE545 amino acid contributions to the electronic interaction between (a) the $PEB_{50/61C}-PEB_{50/61D}$ and (b) the $DBV_{19A}-DBV_{19B}$ chromophore pairs as obtained from atomistic MMPol calculations including the full protein−water system for a representative structure extracted from the molecular dynamics simulation. Images created with VMD.[36]

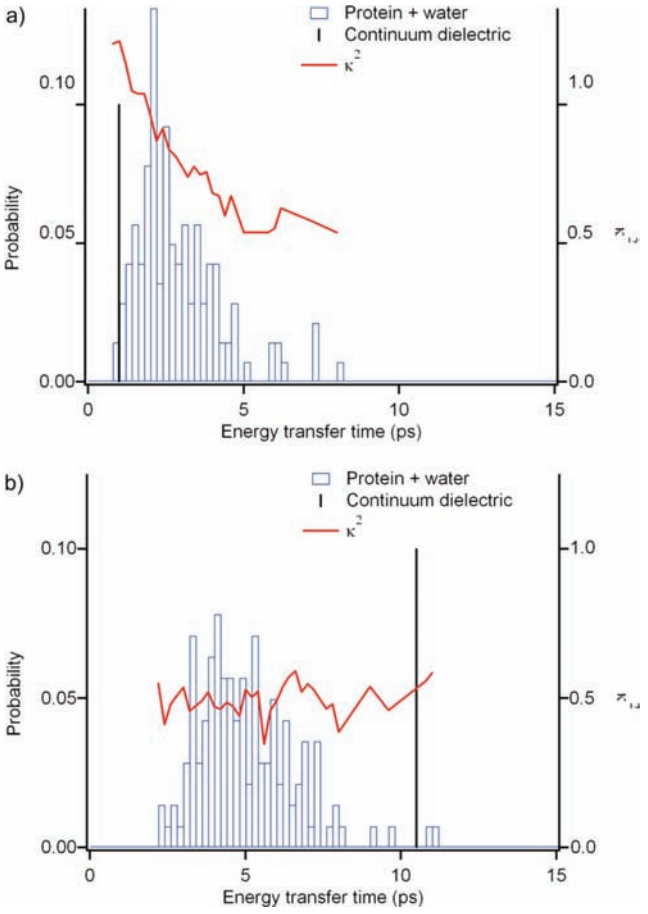

Figure 4. Distribution of times predicted for (a) $PEB_{50/61D} \rightarrow PEB_{50/61C}$ and (b) $DBV_{19A} \rightarrow DBV_{19B}$ energy transfers from electronic couplings calculated from a full atomistic MMPol description of the protein−water system compared to the value obtained from a continuum dielectric description of the environment. The continuum rates are obtained based on the arrangement of the pigments as found in the crystal structure, whereas MMPol rates correspond to structures of the PE545 complex sampled along a classical molecular dynamics simulation. For the latter, corresponding average dipole orientation factors, κ^2, are also displayed.

water solvent, indicates that the variations in the effective dielectric properties are due to the protein structure and not the solvent.

A survey of the results obtained for the different pigment pairs when the isolated protein structure is considered reveals a noteworthy result. The effective permittivity experienced by the $DBV_{19A}-DBV_{19B}$ pair is 0.92. This means that in this particular case the protein does not screen the interaction between these pigments, but instead it enhances it by ∼10%. On the contrary, we find a value of 2.20 for the central $PEB_{50/61C}-PEB_{50/61D}$ pair, which means that this coupling is significantly more attenuated by the protein than the interactions between other pairs. When we also account for the water surrounding the complex, we find that $\langle \varepsilon_{eff} \rangle$ values for these two pairs increase to 1.35 and 2.57 for the DBVs and PEBs pairs, respectively, owing to a further screening effect induced by the solvent. In order to understand the origin of these two cases, we dissected the screening obtained by the MMPol approach into contributions arising from the different residues and waters in the system (see Supporting Information). When the effective permittivity is examined, it is found that some protein regions lead to enhancement and some to screening of the electronic coupling. In Figure 3, we show how the screening calculated by MMPol on a representative MD structure including the full protein−water environment is distributed about the protein residues. If we examine the central $PEB_{50/61C}-PEB_{50/61D}$ pair, the two β polypeptide chains C and D as well as the α chain A of the protein all reduce the interaction by −28%, −15%, and −11%, respectively, whereas the overall effect of chain B is negligible. The waters then add a further −10% screening effect. This is clearly shown in Figure 3, where most residues surrounding the pigments are colored blue according to screening contributions. A completely different picture appears for the peripheral $DBV_{19A}-DBV_{19B}$ pair. In this case, the α subunits that fill the intermolecular space between the chromophores lead to −13% and −20% screening contributions, whereas the β chains induce strong 29% and 21% enhancements of the electronic coupling. This means that the protein is organized in such a way so to increase by 18% the electronic coupling between the DBVs, which translates into a significant increase in the energy transfer rate. The further effect of the surrounding water, however, adds a strong −43% screening contribution, although the net effective permittivity (1.35) is still smaller than that for the other pigment pairs in the complex.

Typically, quantitative models of light harvesting in photosynthetic pigment−protein complexes are derived by calculating the electronic couplings between the pigments from the frozen arrangement of the molecules as found in the crystal structure. In

addition, modulation of these couplings by the environment is described at best by adopting a continuum dielectric model.[8,12,37,38] In Figure 4 we illustrate the new rich picture that appears by considering an atomistic description of the system coupled with a sampling of the conformational space experienced by the complex. In particular, we calculate the energy transfer rates for $DBV_{19A} \rightarrow DBV_{19B}$ and $PEB_{50/61D} \rightarrow PEB_{50/61C}$. The distribution of MMPol rates are obtained using the sets of electronic couplings calculated along the trajectory of the classical MD simulation. For comparison, the continuum energy transfer rates, based on the crystal structure of PE545, are indicated. These energy transfer times are computed in a basis obtained by applying a polaron transformation to the electronic eigenstate basis. All chromophores in the protein are included in the calculation. Details of this method are reported elsewhere.[32]

The small dielectric screening experienced by the DBV_{19A}–DBV_{19B} chromophores in the protein significantly reduces the average energy transfer time (~5 ps) compared to the prediction of the continuum description (~10 ps). The $PEB_{50/61C}$–$PEB_{50/61D}$ molecules, in contrast, experience a high local permittivity ~2.56, thus leading to a transfer time (~3 ps) significantly slower compared to the average dielectric prediction (~1 ps). Overall, we find that energy transfer times between the various pairs of molecules in the PE545 complex are tuned by a factor ranging from 0.3 to 4.3 relative to expectations based on the average dielectric environment (see Supporting Information).

The distribution of transfer times in Figure 4 arises from sizable fluctuations of the electronic interactions between the sites along the trajectory, that is, off-diagonal disorder. Such fluctuations are caused by changes in the relative orientations of the chromophores, as opposed to variations in the interchromophore distances, or the local dielectric permittivities. The dependence of the rates on the orientation factor between the sites is clearly apparent in the distribution of $PEB_{50/61D} \rightarrow PEB_{50/61C}$ rates, as shown in Figure 4. In contrast, the $DBV_{19A} \rightarrow DBV_{19B}$ rates show little dependence on the orientation factor between the two sites. This is perhaps because the DBV_{19A}/DBV_{19B} sites are located on opposite sides of the PE545 complex, and they are coupled through intervening chromophores.[4] Thus the significance of one particular orientation factor is diminished by the interactions with other chromophores.

CONCLUSIONS

In summary, we have shown that the heterogeneous dielectric properties of a light-harvesting protein can profoundly tune (by a factor up to ~4) the energy migration rates between chromophore sites compared to the average continuum dielectric view that has been historically assumed. Clearly, engineering of the local dielectric environment can potentially be used to optimize artificial light-harvesting antenna systems. The key challenge is to control the local environment around each chromophore. In the PE545 complex, the DBV_{19A}–DBV_{19B} interaction is the only one in which the protein actually enhances the coupling between the chromophores. We speculate that the cryptophyte algae have evolved the dielectric structure of PE545 in order to optimize this particular key interaction. It is already the weakest electronic coupling in the complex, yet it is important because it couples the lowest energy chromophores; those that mediate energy transfer to other antenna proteins and ultimately to the photosystems.

ASSOCIATED CONTENT

Supporting Information. Full methods, computational details, and tables of effective dielectric constants, electronic couplings, transition dipole moments, and energy transfer rates. Complete refs 20 and 27. This material is available free of charge via the Internet at http://pubs.acs.org.

AUTHOR INFORMATION

Corresponding Author
carles.curutchet@udg.edu

ACKNOWLEDGMENT

C.C. acknowledges support from the Comissionat per a Universitats i Recerca of the Departament d'Innovació, Universitats i Empresa of the Generalitat de Catalunya, grant no. 2008BPB00108. J.K. thanks the Danish Natural Science Research Council/The Danish Councils for Independent Research for financial support. G.D.S. gratefully acknowledges the Natural Sciences and Engineering Research Council of Canada for financial support. B.M. acknowledges Gaussian Inc. for financial support.

REFERENCES

(1) Cheng, Y. C.; Fleming, G. R. *Annu. Rev. Phys. Chem.* **2009**, *60*, 241.
(2) Engel, G. S.; Calhoun, T. R.; Read, E. L.; Ahn, T. K.; Mancal, T.; Cheng, Y. C.; Blankenship, R. E.; Fleming, G. R. *Nature* **2007**, *446*, 782.
(3) Lee, H.; Cheng, Y. C.; Fleming, G. R. *Science* **2007**, *316*, 1462.
(4) Collini, E.; Wong, C. Y.; Wilk, K. E.; Curmi, P. M. G.; Brumer, P.; Scholes, G. D. *Nature* **2010**, *463*, 644.
(5) Scholes, G. D.; Curutchet, C.; Mennucci, B.; Cammi, R.; Tomasi, J. *J. Phys. Chem. B* **2007**, *111*, 6978.
(6) Curutchet, C.; Scholes, G. D.; Mennucci, B.; Cammi, R. *J. Phys. Chem. B* **2007**, *111*, 13253.
(7) Curutchet, C.; Muñoz-Losa, A.; Monti, S.; Kongsted, J.; Scholes, G. D.; Mennucci, B. *J. Chem. Theory Comput.* **2009**, *5*, 1838.
(8) Novoderezhkin, V. I.; Doust, A. B.; Curutchet, C.; Scholes, G. D.; van Grondelle, R. *Biophys. J.* **2010**, *99*, 344.
(9) Ritchie, R. J. *Photosynth. Res.* **2008**, *96*, 201.
(10) Hammer, A.; Schumann, R.; Schubert, H. *Aquat. Microb. Ecol.* **2002**, *29*, 287.
(11) Iozzi, M. F.; Mennucci, B.; Tomasi, J.; Cammi, R. *J. Chem. Phys.* **2004**, *120*, 7029.
(12) Renger, T. *Photosynth. Res.* **2009**, *102*, 471.
(13) Knox, R. S.; van Amerongen, H. *J. Phys. Chem. B* **2002**, *106*, 5289.
(14) Doust, A. B.; Marai, C. N. J.; Harrop, S. J.; Wilk, K. E.; Curmi, P. M. G.; Scholes, G. D. *J. Mol. Biol.* **2004**, *344*, 135.
(15) Wilk, K. E.; Harrop, S. J.; Jankova, L.; Edler, D.; Keenan, G.; Sharples, F.; Hiller, R. G.; Curmi, P. M. G. *Proc. Natl. Acad. Sci. U.S.A.* **1999**, *96*, 8901.
(16) Onufriev, A.; Gordon, J.; Myers, J.; Anandakrishnan, R.; Folta, T.; Shoja, V.; Heath, L. S.; Shaffer, C.; Back, G.; Rountree, D.; Ruscio, J. Z.; Pevzner, Y. H++ server; Virginia Tech; http://biophysics.cs.vt.edu/H++ (accessed 04/20/09).
(17) Gordon, J. C.; Myers, J. B.; Folta, T.; Shoja, V.; Heath, L. S.; Onufriev, A. *Nucleic Acids Res.* **2005**, *33*, W368.
(18) Anandakrishnan, R.; Onufriev, A. *J. Comput. Biol.* **2008**, *15*, 165.
(19) Jorgensen, W. L.; Chandrasekhar, J.; Madura, J. D.; Impey, R. W.; Klein, M. L. *J. Chem. Phys.* **1983**, *79*, 926.
(20) Case, D. A. et al. *AMBER 9*, University of California: San Francisco, 2006.

(21) Wang, J. M.; Cieplak, P.; Kollman, P. A. *J. Comput. Chem.* **2000**, *21*, 1049.
(22) Hornak, V.; Abel, R.; Okur, A.; Strockbine, B.; Roitberg, A.; Simmerling, C. *Proteins* **2006**, *65*, 712.
(23) Wang, J. M.; Wolf, R. M.; Caldwell, J. W.; Kollman, P. A.; Case, D. A. *J. Comput. Chem.* **2004**, *25*, 1157.
(24) Soderhjelm, P.; Ryde, U. *J. Phys. Chem. A* **2009**, *113*, 617.
(25) Gagliardi, L.; Lindh, R.; Karlstrom, G. *J. Chem. Phys.* **2004**, *121*, 4494.
(26) Karlstrom, G.; Lindh, R.; Malmqvist, P. A.; Roos, B. O.; Ryde, U.; Veryazov, V.; Widmark, P. O.; Cossi, M.; Schimmelpfennig, B.; Neogrady, P.; Seijo, L. *Comput. Mater. Sci.* **2003**, *28*, 222.
(27) Frisch, M. J. et al. *Gaussian 09, Revision A.2*; Gaussian, Inc.: Wallingford, CT, 2009.
(28) Nielsen, C. B.; Christiansen, O.; Mikkelsen, K. V.; Kongsted, J. *J. Chem. Phys.* **2007**, *126*, 154112.
(29) Tomasi, J.; Mennucci, B.; Cammi, R. *Chem. Rev.* **2005**, *105*, 2999.
(30) Jordanides, X. J.; Lang, M. J.; Song, X. Y.; Fleming, G. R. *J. Phys. Chem. B* **1999**, *103*, 7995.
(31) Rappe, A. K.; Casewit, C. J.; Colwell, K. S.; Goddard, W. A.; Skiff, W. M. *J. Am. Chem. Soc.* **1992**, *114*, 10024.
(32) Hossein-Nejad, H.; Curutchet, C.; Kubica, A.; Scholes, G. D. *J. Phys. Chem. B* **2011**, DOI: 10.1021/jp108397a.
(33) Pereverzev, A.; Bittner, E. R. *J. Chem. Phys.* **2006**, *125*, 104906.
(34) We note here that the chromophore−chromopore distances averaged along the MD trajectory differ in all cases by less than 1.4 Å with respect to the crystal structure. Therefore, performing continuum calculations on MD structures other than the crystal would introduce no significant differences in the values of effective dielectric permittivities obtained.
(35) Hansen, T.; Jensen, L.; Astrand, P. O.; Mikkelsen, K. V. *J. Chem. Theory Comput.* **2005**, *1*, 626.
(36) Humphrey, W.; Dalke, A.; Schulten, K. *J. Mol. Graph.* **1996**, *14*, 33.
(37) Adolphs, J.; Renger, T. *Biophys. J.* **2006**, *91*, 2778.
(38) Mirkovic, T.; Doust, A. B.; Kim, J.; Wilk, K. E.; Curutchet, C.; Mennucci, B.; Cammi, R.; Curmi, P. M. G.; Scholes, G. D. *Photochem. Photobiol. Sci.* **2007**, *6*, 964.